

SUPPLEMENTAL MATERIAL

Table S1. Baseline characteristics of mice.

		Lower 95% CI	Upper 95% CI
Number of mice (<i>n</i>)	6	-	-
Age (weeks)	24-26	-	-
Sex	Females	-	-
Mouse strain	C57BL/6	-	-
Avg. 2 nd MCA branch diameter (μm)	34.02	28.16	39.87
Avg. 2 nd MCA branch blood flow (BFI)	482	242	722
Density of perfused capillaries (pr. 0.0324 mm ³)	202	182	222

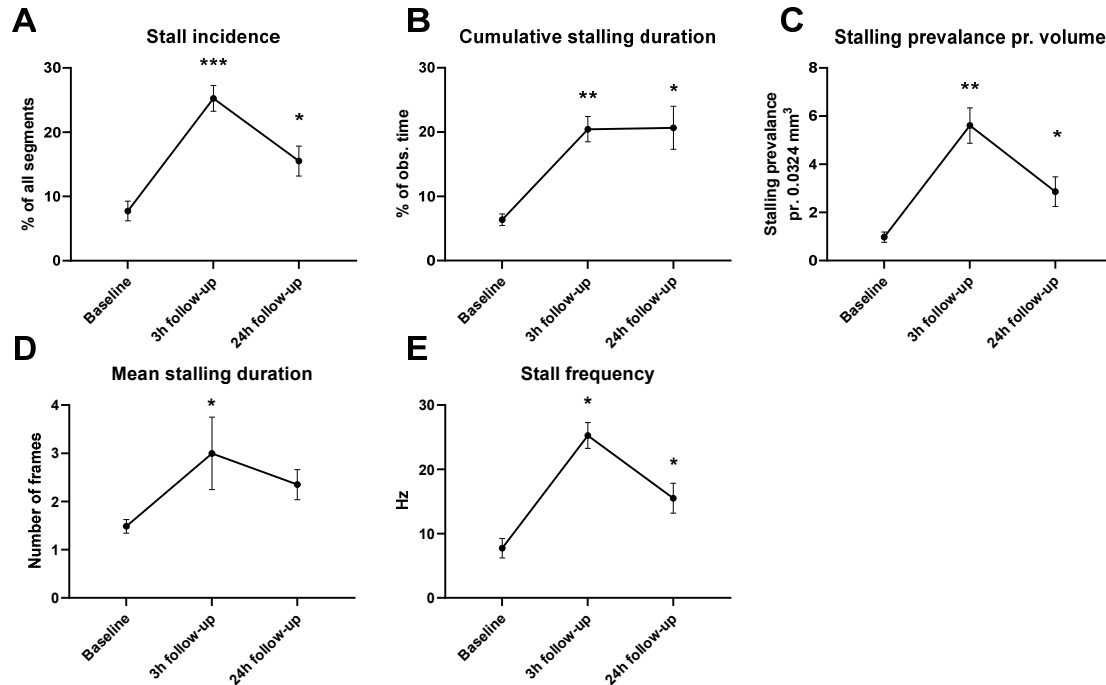
The diameter and blood flow index (BFI) of the middle cerebral artery (MCA) were assessed using optical coherence tomography and laser speckle contrast imaging, respectively. CI, confidence interval.

Table S2. Properties of spreading depolarizations during arterial occlusion.

	Mean \pm SEM	Lower 95% CI	Upper 95% CI
Spreading depolarization propagation velocity (mm/min)	4.16 \pm 0.21	3.61	4.71
Time from beginning of occlusion to first spreading depolarization (sec)	143.30 \pm 32.01	61.06	225.6
Initial spreading depolarization hypoperfusion duration (sec)	36.25 \pm 1.25	32.27	40.23
Amplitude of initial spreading depolarization hypoperfusion (%)	-33.60 \pm 6.01	-52.71	-14.48
Spreading depolarization hyperperfusion duration (sec)	96.38 \pm 6.67	79.24	113.50
Amplitude of spreading depolarization hyperperfusion (%)	72.49 \pm 10.59	45.28	99.70
Number of spreading depolarizations during 60 min occlusion	11.33 \pm 1.86	6.56	16.10

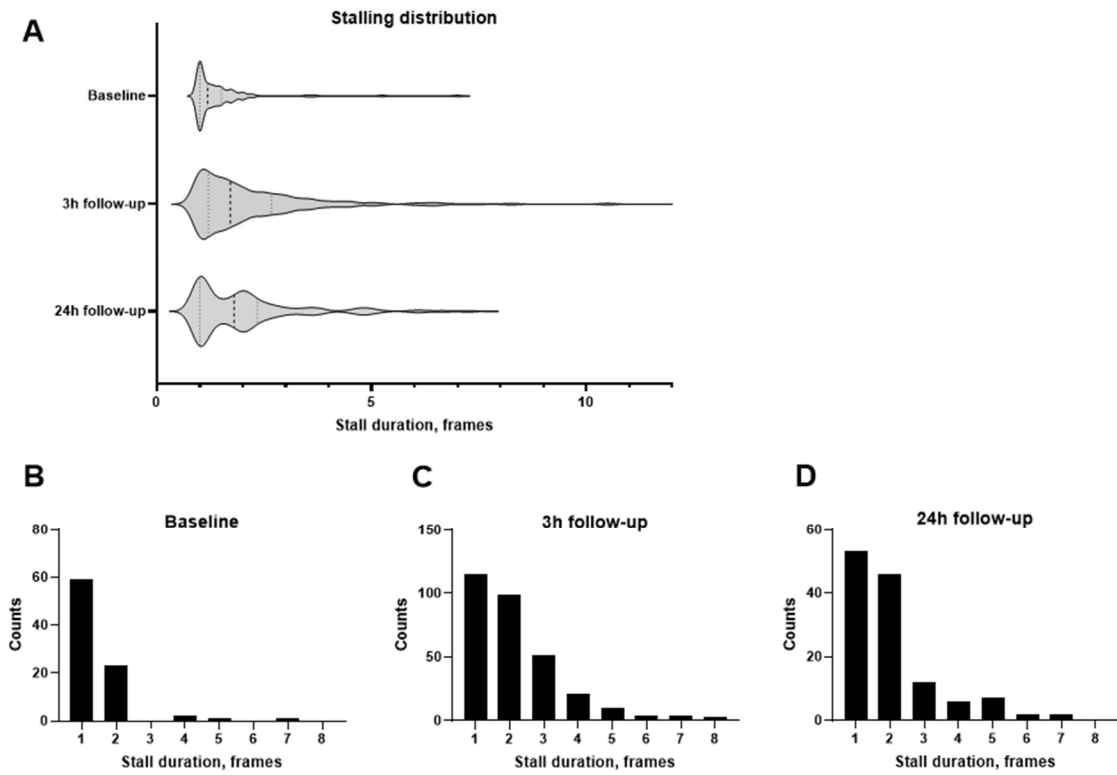
The first spreading depolarization in each mouse led to initial hypoperfusion followed by a wave of hyperperfusion and subsequently sustained hypoperfusion. The subsequent spreading depolarizations during the sustained hypoperfusion were associated with a wave of hyperperfusion. Peak amplitude was calculated as the maximal change in blood flow during spreading depolarization compared to an average of flow 1 min preceding the spreading depolarization. See Fig. 2 for representative traces and Video S1. CI, confidence interval. $n=6$.

Figure S1. Dynamic capillary flow stalling was increased after reperfusion.



A, The incidence of capillary flow stalling was increased at the 3 and 24h follow-up compared with baseline. **B**, Cumulative stalling duration was increased at the 3 and 24h follow-up compared with baseline. **C**, Stalling prevalence normalized to the field of view, i.e., 600x600x90 μm , was increased at the 3 and 24h follow-up compared with baseline (point prevalence normalized to the number of perfused capillaries is shown in Fig. 5F). **D**, The mean stalling duration was increased at the 3h follow-up, but not statistically different 24h after reperfusion compared with baseline. **E**, The mean stalling frequency of capillary segments that exhibited stalling was increased at the 3 and 24h follow-up compared with baseline. Error bars as standard error. Data were compared with baseline using repeated measures 1-way ANOVA followed by Dunnett's multiple comparisons test. *, **, *** $P < 0.05, 0.01, 0.001$; $n = 6$.

Figure S2. Frequency distribution of mean duration of each capillary stalling.



A, Distribution of stalling durations for all capillary stallings as a violin plot. Histograms show the frequency distribution of stalling durations at baseline (**B**), 3h (**C**) and 24h follow-up (**D**). Optical coherence tomography framerate=0.167 Hz. $n=6$.

Figure S3. Point prevalence, stallogram, and Pearson correlation plot for each mouse.

Left panel: Traces of point prevalence of capillary flow stalling (y-axis) is shown for each frame (x-axis) and suggests that capillary stalls are not rhythmic at baseline nor after reperfusion.

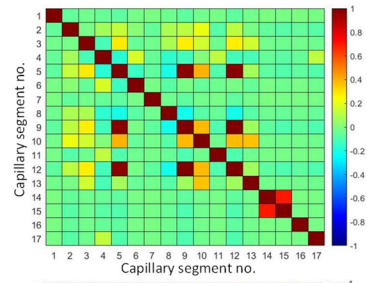
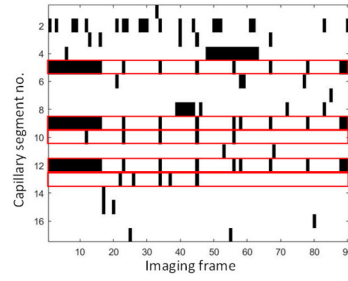
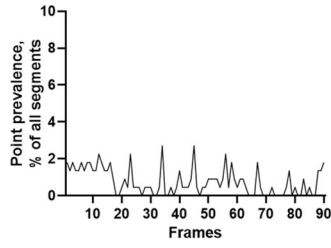
Middle panel: Stallograms in the middle panel showing the timeline of stalling capillary segments through the 90 consecutive angiograms where black indicates capillary stalling.

Right panel: Pearson correlation analysis of capillary stalls suggested that capillary stalling is not synchronized. One exception was a group of spatially related capillaries in mouse #1 that exhibited synchronized and rhythmic stalling, which is indicated with red rectangles in the stallograms. The rhythmic stalls are also shown in Video S3.

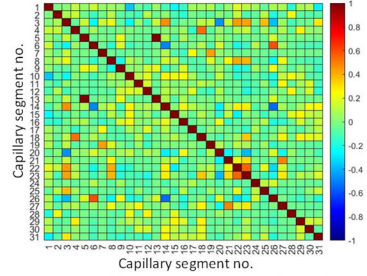
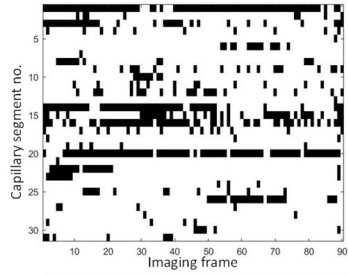
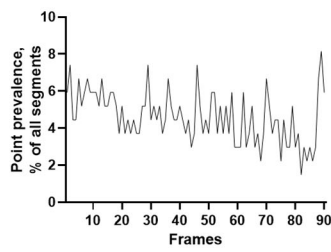
Figure S3

Mouse #1

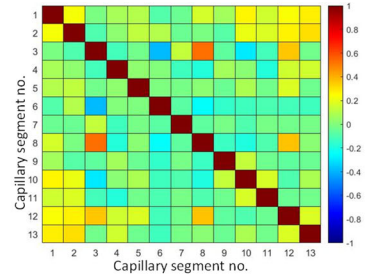
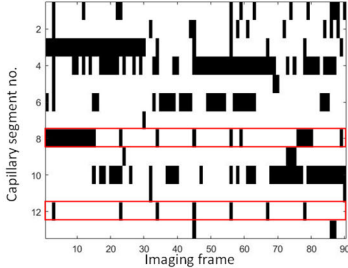
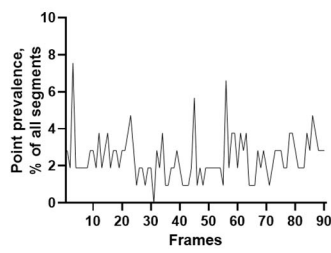
Baseline



3h follow-up

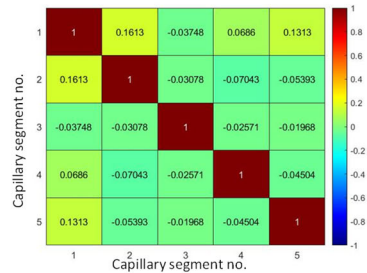
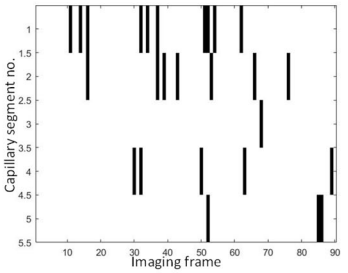
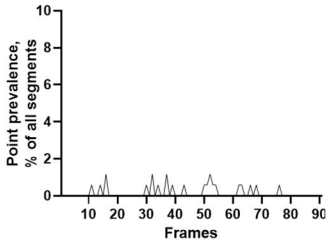


24h follow-up

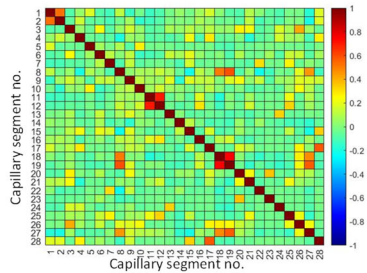
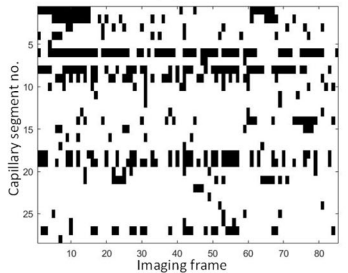
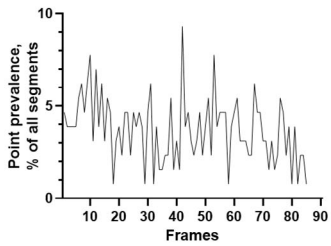


Mouse #2

Baseline



3h follow-up



24h follow-up

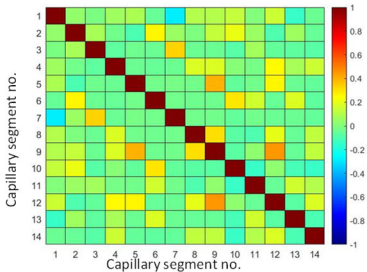
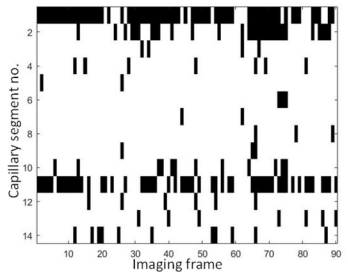
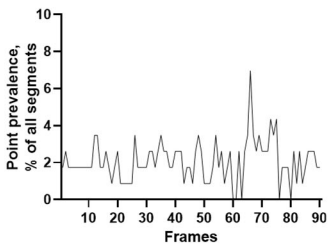
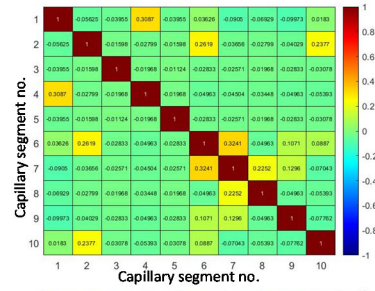
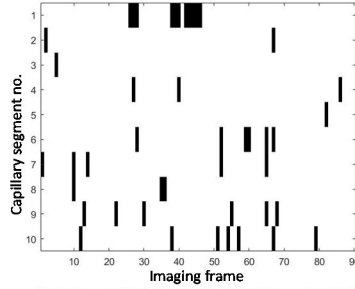
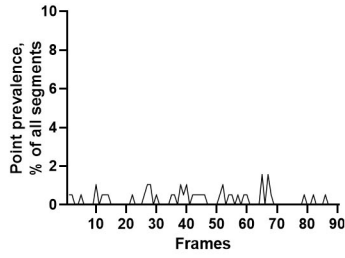


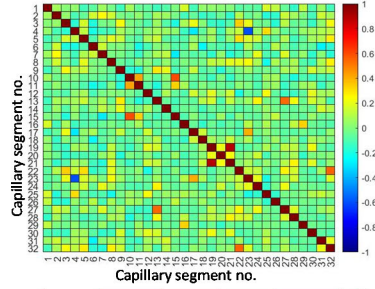
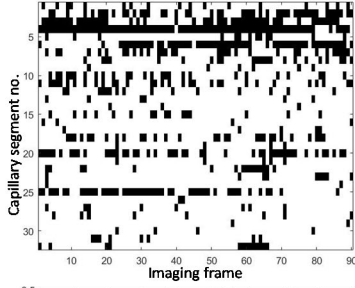
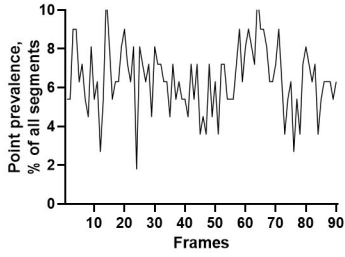
Figure S3, continued

Mouse #3

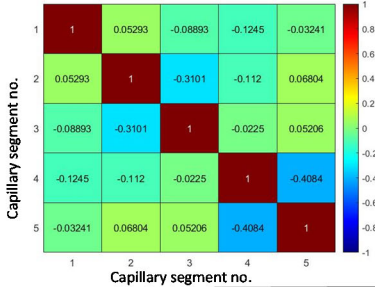
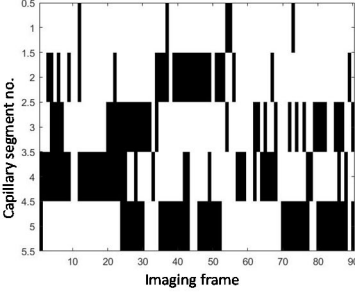
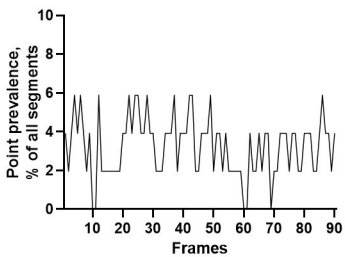
Baseline



3h follow-up

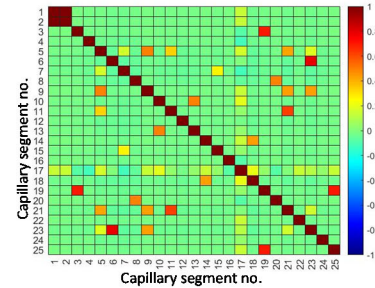
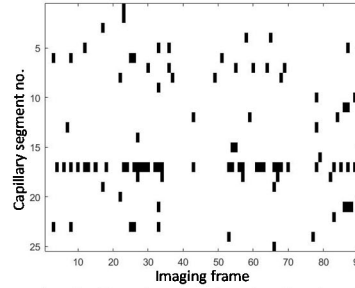
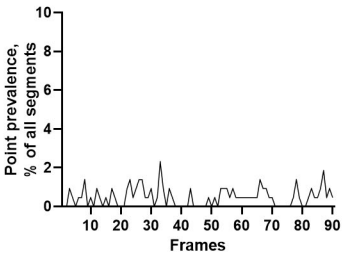


24h follow-up

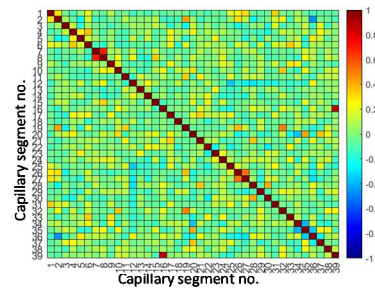
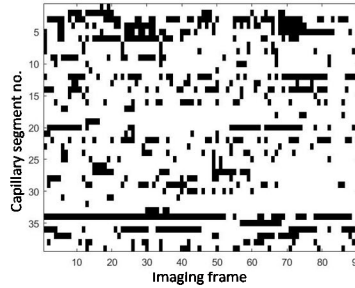
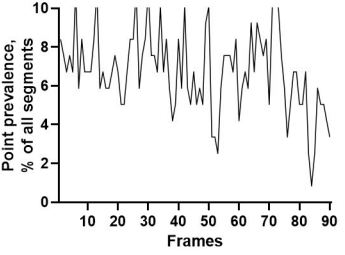


Mouse #4

Baseline



3h follow-up



24h follow-up

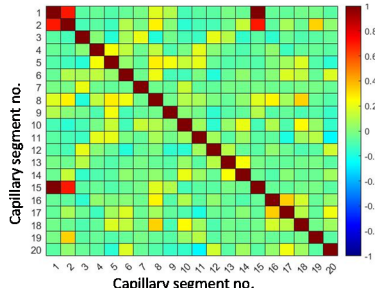
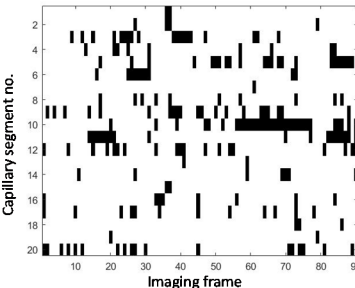
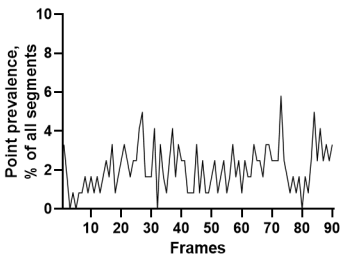
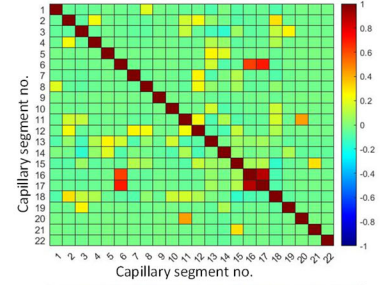
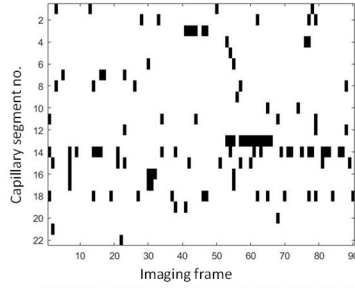
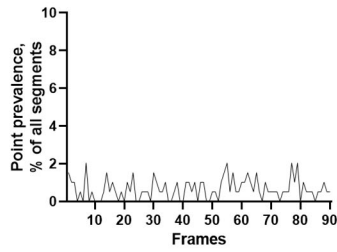


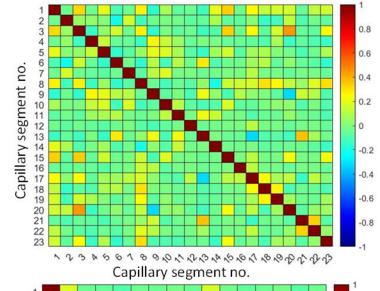
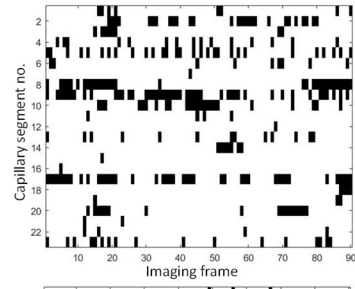
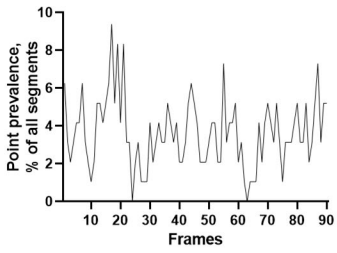
Figure S3, continued

Mouse #5

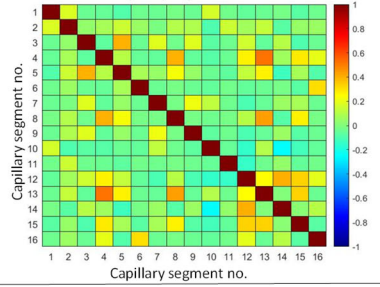
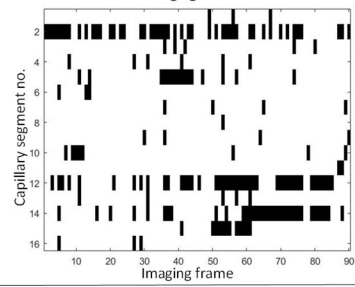
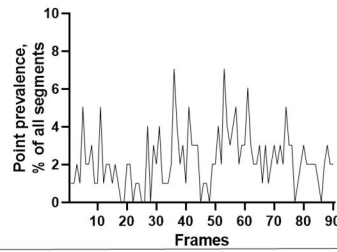
Baseline



3h follow-up

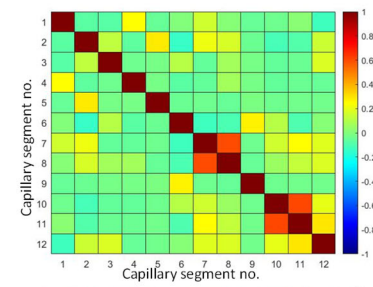
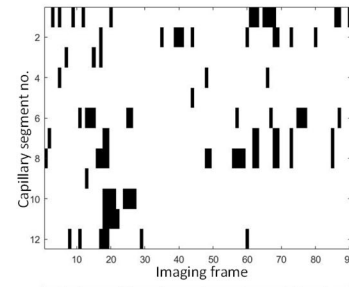
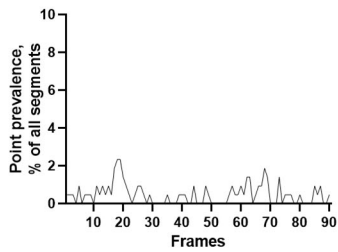


24h follow-up

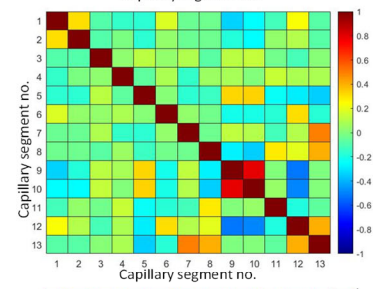
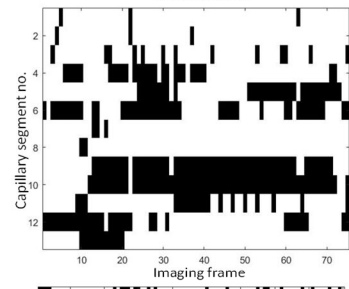
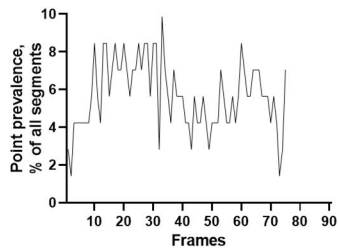


Mouse #6

Baseline



3h follow-up



24h follow-up

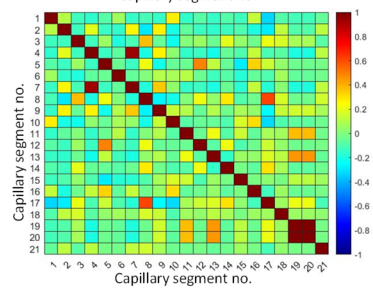
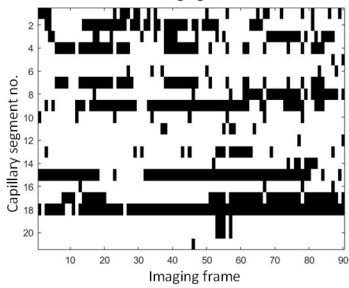
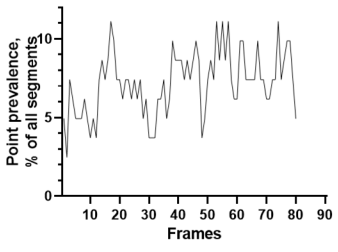
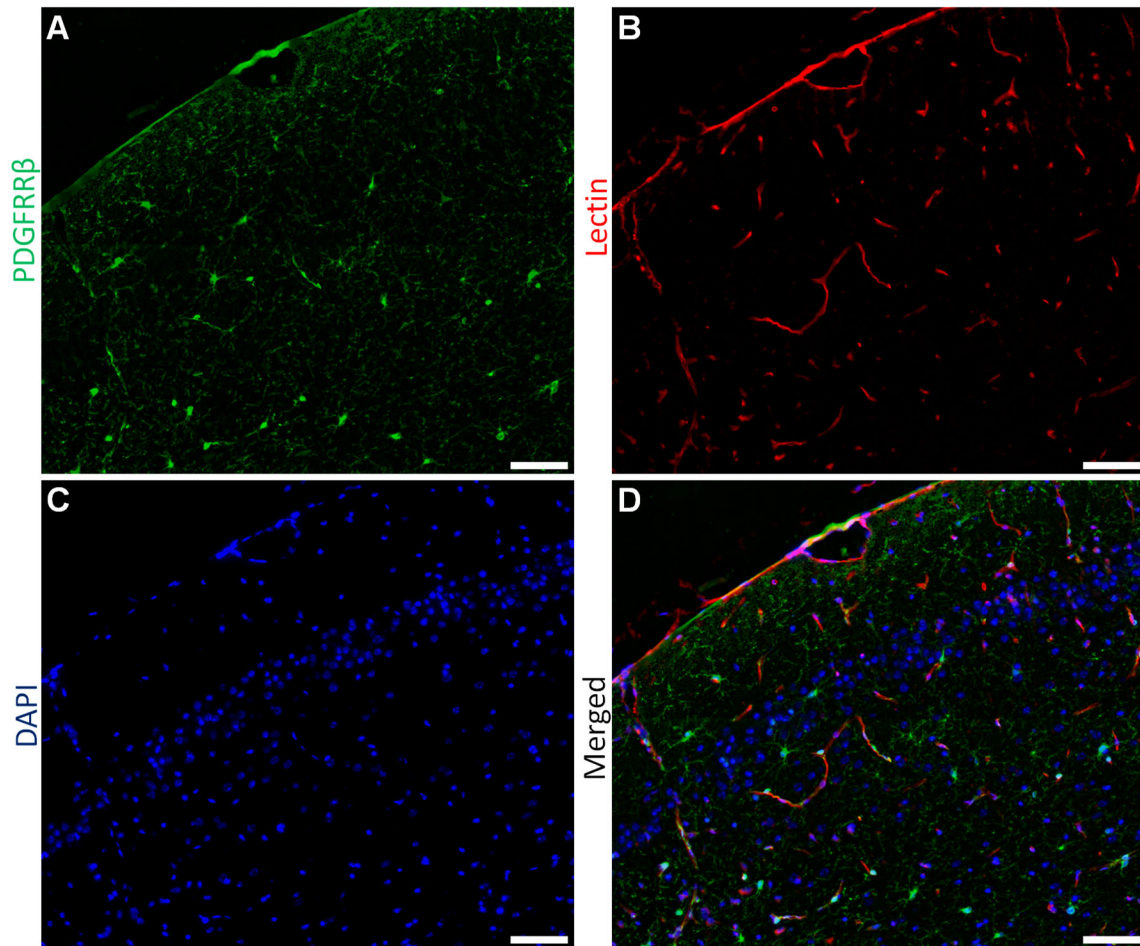


Figure S4. Representative pericyte and endothelium labelling in peri-ischemic tissue.



Tissue was perfusion-fixed at the 24h follow-up and pericytes and endothelium labelled with platelet derived growth factor receptor β (PDGFR β ; **A**; green), and lectin (**B**; red), respectively; and nuclei highlighted with 4',6-diamidino-2-phenylindole (DAPI; **C**; blue). **D**, Spatial relationships of the three labels are shown in the triple merged image. Bars, 100 μ m. See Fig. 7 for statistical analysis.

Video S1. Laser speckle contrast imaging during arterial occlusion. Laser speckle contrast imaging ensured no-flow in the targeted artery during the 1h occlusion. The top left panel shows absolute blood flow index (BFI) in each pixel. The top right panel shows overlay of BFI values at the given time point relative to baseline. Only BFI changes exceeding the threshold of $\pm 25\%$ are overlaid as specified by the color bar on the right side to show relevant BFI changes. Relative changes in blood flow (right panel) show the drop in blood flow downstream from the targeted artery. The baseline in the right panel is reset at 4 minutes and 10 seconds (as indicated 10 seconds into the video) to highlight the changes in BFI after the first spreading depolarization (SD). Multiple spreading depolarizations propagated through the peri-ischemic cortex during the arterial occlusion. This was associated with a drop in BFI in the peri-ischemic cortex. The bottom panel presents mean BFI over time in the three corresponding color-coded regions of interest.

Video S2. Increased capillary flow stalling after reperfusion. Capillary flow stalling was assessed by optical coherence tomography angiograms. Representative angiograms are shown at baseline (left) and 3h after reperfusion (right). Capillary flow stallings as indicated with arrows.

Video S3. Rhythmic and synchronized capillary flow stalling. In one mouse, a group of capillaries showed rhythmic stalling with a frequency of approximately 0.1 Hz. Capillary flow dynamics were assessed by optical coherence tomography angiography. Video speed x30. Stalling data from this mouse is shown in Figure S3, indicated Mouse #1.